Available online at www.sciencedirect.com
ScienceDirect
Ceramics International 36 (2010) 1327–1338
CERAMICS INTERNATIONAL
www.elsevier.com/locate/ceramint

Investigation of the effect of ZrO_2 and ZrO_2/Al_2O_3 additions on the hot-pressing and properties of equimolecular mixtures of α- and β-Si_3N_4

E.M.M. Ewais [a,*], M.A.A. Attia [b], A. Abousree-Hegazy [b], R.K. Bordia [c]

[a] *Refarctory & Ceramic Materials Lab (RCML), Central Metallurgical R&D Institute, P.O. Box 87 Helwan, Cairo, Egypt*
[b] *Mechanical Engineering Department, Faculty of Engineering, Helwan University, P.O. Box 11792 Helwan, Cairo, Egypt*
[c] *Department of Materials Science and Engineering, University of Washington, Roberts Hall, Seattle, WA 98195, USA*

Received 28 April 2009; received in revised form 27 November 2009; accepted 3 January 2010
Available online 29 January 2010

Abstract

In this work, hot-pressing of equimolecular mixtures of α- and β-Si_3N_4 was performed with addition of different amounts of sintering additives selected in the ZrO_2–Al_2O_3 system. Phase composition and microstructure of the hot-pressed samples was investigated. Densification behavior, mechanical and thermal properties were studied and explained based on the microstructure and phase composition. The optimum mixture from the ZrO_2–Al_2O_3 system for hot-pressing of silicon nitride to give high density materials was determined. Near fully dense silicon nitride materials were obtained only with the additions of zirconia and alumina. The liquid phase formed in the zirconia and alumina mixtures is important for effective hot-pressing. Based on these results, we conclude that pure zirconia is not an effective sintering additive. Selected mechanical and thermal properties of these materials are also presented. Hot-pressed Si_3N_4 ceramics, using mixtures from of ZrO_2/Al_2O_3 as additives, gave fracture toughness, K_{IC}, in the range of 3.7–6.2 MPa $m^{1/2}$ and Vicker hardness values in the range of 6–12 GPa. These properties compare well with currently available high performance silicon nitride ceramics. We also report on interesting thermal expansion behavior of these materials including negative thermal expansion coefficients for a few compositions.

Keywords: A. Hot-pressing; D. Si_3N_4; D. ZrO_2; D. Al_2O_3; C. Mechanical properties; C. Thermal properties; Microstructure

1. Introduction

Low porosity non-oxide ceramics Si_3N_4, AlN, B_4C, BN and SiC ceramics are attracting materials. This is due to their potential uses as a high temperature engineering materials substituting structural metals. Many of the non-oxide ceramics have attractive mechanical properties (strength, hardness, wear resistance) and unique combinations of thermal and electrical conductivity. Finally, some of them have high thermal shock resistance and are chemically stable in a variety of harsh environments.

Silicon nitride is one of the most promising of advanced ceramic materials. It is also the most extensively studied ceramic for high temperature applications. This is because of its low density, high temperature strength, excellent thermal shock resistance and better reliability compared to other ceramics. Some of the common applications of silicon nitride include cutting tools, bearings, reciprocating engine parts, wear and metal forming components and springs [1–11]. Transportation related applications include automotive valves, turbocharger rotors and valve guides. Silicon nitride parts contribute to the reduction in emissions and increase in the efficiency of engines and in enhancing the productivity in variety of metal working processes. As result, an estimated global market for silicon nitride is expected to reach $700 million in the near future [12].

Despite the impressive material properties of silicon nitride, e.g. high strength and thermal shock resistance, good corrosion and wear resistance, its commercial use has been quite limited. The major obstacle to large-scale implementation has been the high manufacturing cost. In addition, the performance of the objects manufactured from silicon nitride is controlled by the amount and type of sintering aids. These additives must be added to enable liquid phase sintering (LPS) to high density, but if the amount of additives can be reduced or if the additives have unique mechanical and thermal properties while maintaining good sintering properties, the performance of the silicon nitride

* Corresponding author.
E-mail address: dr_ewais@hotmail.com (E.M.M. Ewais).

0272-8842/$36.00
doi:10.1016/j.ceramint.2010.01.018

can be significantly improved. In addition, the brittleness of silicon nitride is considered one of its main drawbacks that limit its application. However, many approaches have been proposed to improve the fracture toughness of Si_3N_4 [13–17].

The mechanical properties depend on several variables. Chief among these is powder characteristics. Powders with high α content have usually been used as the starting material since the sintered Si_3N_4 body consists of a composite-like microstructure due to the α–β phase transformation. It has been reported that the large, elongated β grains with high-aspect-ratio deflect the propagation of cracks, thus increasing the fracture toughness of the material. However, large grains may act as crack origin lowering the flexural strength of the sintered material. So, it is important to control the amount and aspect ratio of the large β-grains in order to improve the mechanical properties of silicon nitride materials [18–26]. Xu et al. [19] reported that the mechanical properties have an optimum if the α/β ratio equals 1 in the starting material mixture.

Since the densification of Si_3N_4 plays an important role in the cost of Si_3N_4 production, significant effort has been made to optimize the densification via liquid phase. It was reported that part of densification can be achieved by the rearrangement of Si_3N_4, particles induced by the formation of liquid phase due to reaction between the SiO_2 layer (typically 0.5–3 wt.%) present on the surface of starting α-Si_3N_4 powders and the sintering aids. Complete densification can be achieved through reactive liquid phase sintering mechanism. The α-Si_3N_4, particles dissolve in the liquid and precipitate as β-Si_3N_4, via a reconstructive phase transformation. While sintering continues, the β-Si_3N_4, nuclei grow as elongated grains and form an interlocked grain structure [9,15,16,18,24,27–38]. It has been noted that fully dense objects cannot be produced without the use of sintering additives. As previously mentioned, the type and amount of sintering additives determine the nature and the properties of liquid formed [9,15,16,18,23,27–32]. Al_2O_3, Y_2O_3, MgO, AlN as well as rare earth oxides have been used as sintering additives for silicon nitride. Al_2O_3 and Y_2O_3 are considered the most common sintering additives but Y_2O_3 is expensive [13,15,23,28,38–42]. Fisher et al. [14] reported that an alternative cheaper sintering additive would help to reduce the cost of producing Si_3N_4 ceramics. ZrO_2 is a possible replacement for Y_2O_3. It has been reported that ZrO_2 is an effective and attractive additive for hot-pressing Si_3N_4 ceramics [43], as it has the potential of toughening and strengthening Si_3N_4-based ceramic materials. It also improves the oxidation resistance due to the presence of more refractory grains boundary phases [44]. However, using a stabilizing agent such as Y_2O_3 (>4.1 mmol%) or CeO_2 (~3.81 mol%) is very important to reduce or prevent the nitrogen uptake by ZrO_2 during densification of Si_3N_4–ZrO_2 composites [45]. It was also reported that addition of MgO to Si_3N_4–ZrO_2 system plays an important role as a sintering agent and stabilization of ZrO_2 [46]. Thus the fabrication of silicon nitride based ceramics in the presence of zirconia have to have a stabilizing agent when the processing is conducted in nitrogen atmosphere [47].

Several investigators have studied the Si_3N_4–ZrO_2 composite system [48,49]. In these studies pressureless-sintering of this system under nitrogen overpressure at temperatures of 1800 °C and 2140 °C was carried out. Results indicated that 20 vol% ZrO_2 (i.e. ~30 wt.%) should be added to form—high-density materials. To improve the fracture toughness of Si_3N_4, the content of ZrO_2 should be in the range of 15–20 wt.%. About 20 wt.% Y_2O_3–stablized ZrO_2 (3 mol% Y_2O_3) with small amounts of Al_2O_3 (1–4 wt.%) and/or Y_2O_3 (2–6 wt.%) was used as sintering aid at 1775 °C. Hot-isostatic pressing of Si_3N_4–ZrO_2 composite at 1550 and 1750 °C using both unstabilized and stabilized ZrO_2 (3 mol% Y_2O_3) gave fully dense objects with addition of >1 wt.% Al_2O_3 or >4 wt.% Y_2O_3. This investigation mentioned that hot-isostatic pressed (HIP) composite at low temperature was harder compared to higher temperature. In addition, Si_3N_4 formed with 2–6 wt.% of ZrO_2 with simultaneous addition of 2–6 wt.% Y_2O_3 and 2–4 wt.% Al_2O_3 densified at 1750 °C and showed a good combination of Vicker hardness (HV10) and indentation fracture toughness. Therefore, addition of stabilizing agent to Si_3N_4–ZrO_2 composite and sintering at high temperature must be considered.

On the other hand, composites in ZrO_2–Al_2O_3 system have the potential to combine an increased hardness with excellent toughness of tetragonal zirconia. In addition, several compositions are well-known as candidates for high temperature applications. One of the attractive points in this system is the formation of eutectic composition at 1710 ± 10 °C in ZrO_2–Al_2O_3 [50]. Therefore, exploitation of the eutectic composition as liquid phase sintering should be considered in the densification process.

In this paper, we present our systematic results on the processing and properties of equimolecular mixtures of α- and β-Si_3N_4 with cost effective ZrO_2 and ZrO_2/Al_2O_3 as densification additives.

2. Experimental procedures

2.1. Materials

The starting powders used in this study were α- and β-Si_3N_4 powders (FUJIAN SINOCERA ADVANCED MATERIAL CO., Ltd., China). Zirconia (zirconia-TZ-3Y) was obtained from Tosoh Ceramics Deviation (NJ, USA). The powder contains 5 wt.% yttria for stabilization of the tetragonal phase. Pure (99.99%) chemical-grade Al_2O_3 powder (GPR) was supplied by Arabic Scientific Office (Egypt). Details of these powders are given in Tables 1 and 2.

Table 1
Particle size distribution of the starting powders.

	α-Si_3N_4, μm	β-Si_3N_4, μm	ZrO_2, μm	Al_2O_3, μm
d_{10}	0.29	0.59	5	3.3
d_{50}	1.24	2.04	0.7	4.65
d_{90}	2.43	4.83	0.2	5.75

Table 2
Chemical composition analysis of the starring powders.

	α-Si_3N_4, wt.%	β-Si_3N_4, wt.%		ZrO_2, wt.%	Al_2O_3, wt.%
N	37.6	37.5	ZrO_2	94.12	–
Si	59.5	59.6	Y_2O_3	5.17	–
O	1.4	1.4	Al_2O_3	0.005	99.98
Fe	0.2	0.2	Fe_2O_3	0.002	–
C	0.08	0.09	SiO_2	0.005	–
			Na_2O	0.021	–
			L.O.I.	0.680	–

2.2. Hot-pressing

Two groups of batches from silicon nitride powders (α- and β-Si_3N_4) and their additives were prepared. Group (I) was α- and β-Si_3N_4 powders with weight ratio α/β = 1 and mixed with zirconia. Group (II) was α- and β-Si_3N_4 powders with weight ratio α/β = 1 mixed with different ratios of zirconia/alumina. The composition of the two group batches are given in Table 3. The powders for each batch were mixed and grounded in planetary mill for 6 h. The mixed powder was then preformed into a rectangle, 35 mm × 6.5 mm × 7.5 mm. Subsequently, these performs were hot-pressed at 1800 °C for 20 min under pressure of 30 MPa in CO/CO_2 atmosphere where the partial pressure of carbon monoxide was higher than carbon dioxide ($P_{CO} > P_{CO_2}$). The hot-pressing of the powders was conducted in a rectangular high-density graphite die coated by boron nitride (BN). The heating rate and cooling rates were 100 °C/min and 50 °C/min respectively. The load was applied from the beginning of heating and stopped at the beginning of cooling.

2.3. Characterization

Densification parameters in terms of bulk density and apparent porosity of the fired samples were determined according to JIS R2205-1974. The development of phases after sintering was followed using X-ray diffraction (D8 Advanced Bruker AXS, GMbH, Karlsruhe, Germany). Fracture and polished surfaces of the specimens were investigated using Scanning Electron Microscope (SEM, Model JSM-5410, JEOL, Tokyo, Japan) with electron dispersive spectroscopy (EDS). Such investigations were performed to identify the sample textures, phases and their distribution. From these data, it is possible to understand the behavior of the samples after sintering and their correlation with changes of the sintering parameters.

Macrohardness and fracture toughness values have been determined, at room temperature, on the polished surface considering an average of five indentation using Vickers indentation method [51–61] with 20 kg load for 15 s. The crack paths, introduced by Vickers indentation with 20 kg load, were investigated in order to evaluate toughening mechanisms. Calculation of the fracture toughness "K_{IC}" was carried out based on the nature of cracks observed. In case of *Palmqvist* cracks, K_{IC} was calculated based on the Palmqvist shaped-crack model using the following relation:

$$K_{IC} = \frac{0.0515P}{C^{3/2}}.$$

However, for the case of *halfpenny* cracks, K_{IC} was calculated based on the half-penny shaped-crack model using the following relation:

$$K_{IC} = \frac{0.0726P}{C^{3/2}}$$

where C the crack length measured from the middle of the Vickers indentation (m). P is the indentation load (N). K_{IC} is the fracture toughness (MPa $m^{1/2}$).

Linear thermal expansion (TE) and its coefficient (CTE) of the hot-pressed samples was measured using dilatometer (Linseis Inc., Germany, Model L76/1550) in the temperature range of room temperature up to 1200 °C with a heating rate of 10 °C/min.

3. Results and discussions

3.1. Phase evolution and microstructural characterization

Fig. 1 shows the X-ray diffraction of hot-pressed silicon nitride mixtures of group (I) which contains 5–20 wt.%

Table 3
The composition of the first and second group batches.

Composition of batches, wt.%					
Batch code		α-Si_3N_4	β-Si_3N_4	ZrO_2	Al_2O_3
Group (I)	SN	50	50		–
	SNZ5	47.5	47.5	5	–
	SNZ10	45	45	10	–
	SNZ15	42.5	42.5	15	–
	SNZ20	40	40	20	–
Group (II)	SNZA1	45	45	5	5
	SNZA2	40	40	10	10
	SNZA3	45	45	3.33	6.67
	SNZA4	40	40	6.67	13.33
	SNZA5	45	45	6.67	3.33
	SNZA6	40	40	13.33	6.67

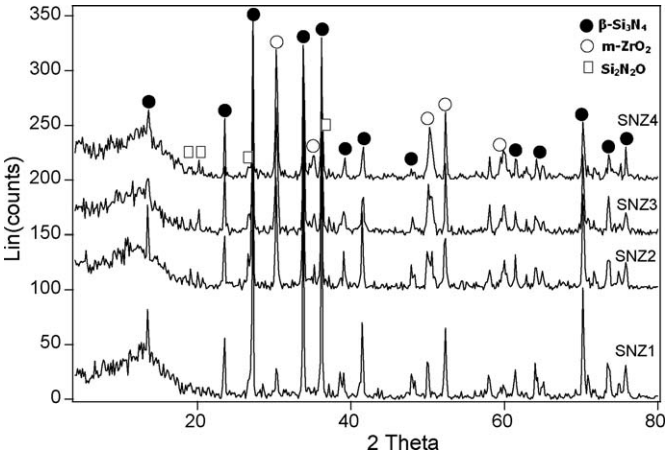

Fig. 1. X-ray diffraction patterns of the hot-pressed Si_3N_4–ZrO_2 mixtures.

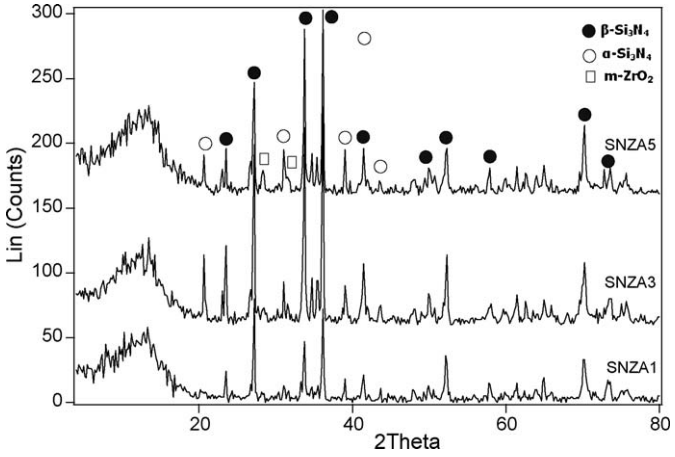

Fig. 2. X-ray diffraction patterns of the hot-pressed Si_3N_4 containing 10 wt.% of ZrO_2/Al_2O_3 mixtures of ratio of 1, 0.5 and 2.

zirconia. Generally, the XRD analysis does not reveal any peaks for α-Si_3N_4. The main crystalline phases shown by this analysis are β-silicon nitride, monoclinic zirconia (m-ZrO_2) and small amounts of silicon oxy-nitride (Si_2N_2O). This means that α-silicon nitride is completely transformed into β-silicon nitride. Formation of Si_2N_2O indicates two reaction possibilities [62–72]. First, capturing the oxygen from zirconia and reaction with silicon nitride. Second, the reaction of the silica (SiO_2) layer that exists on the silicon nitride according to the equation

$$Si_3N_4 + SiO_2 \rightarrow 2Si_2N_2O$$

The XRD of hot-pressed silicon nitride mixtures of group (II) which contains 10 and 20 wt.% zirconia(Z)/alumina(A) of different ratios (1, 0.5 and 2) are shown in Figs. 2 and 3. The XRD analysis revealed that the mixtures composed mainly of α- and β-Si_3N_4 as the major crystalline phases and small amounts of m-ZrO_2. However, the relative intensity of β-Si_3N_4 phase is higher than α-Si_3N_4. This indicated that some α-Si_3N_4 transformed into β-Si_3N_4 during the sintering process. This result matches with published reports [15,28,38,42,73]. In the investigated system, the zirconia detected is not proportional

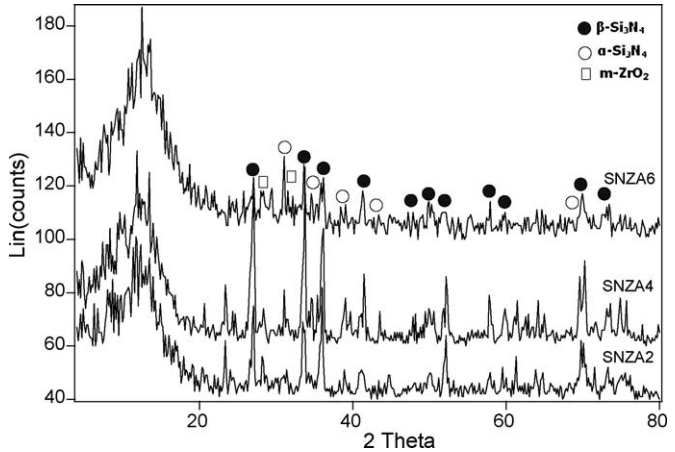

Fig. 3. X-ray diffraction patterns of the hot-pressed Si_3N_4 containing 20 wt.% of ZrO_2/Al_2O_3 mixtures of ratio of 1, 0.5 and 2.

with its quantity added; in addition, alumina peaks are not detected. This is due to the reaction of a part of the zirconia with alumina forming liquid phase at the processing temperature according to the Al_2O_3–ZrO_2 phase diagram. The disappearance of alumina (for all cases) and presence of the amorphous phases is evidence that liquid phases between alumina and zirconia is formed. By increasing the content of zirconia and alumina to 20 wt.% (at all Z/A ratios), the relative intensity of the all crystalline phases decreased (α- or β-Si_3N_4 or m-ZrO_2) and the system proceeds towards higher amount of amorphous phases.

It was obvious that a part of α-Si_3N_4 was retained without transformation into β-Si_3N_4; this may be related to the insufficient holding time [33,36,74]. However, in case of the investigation of the hot-pressed silicon nitride samples of group I that contain zirconia only, α-Si_3N_4 was completely transformed at the same holding time. This means that the holding time is not the only factor that controls the transformation process. The chemistry of liquid phases formed must be important for this transformation.

The investigation of the fracture surface of the hot-pressed SNZ10 and SNZ20 of group (I) using Scanning Electron Microscope shows elongated silicon nitride grain as shown in Fig. 4. Also, a few elongated Si_3N_4 grains embedded in a fine grain Si_3N_4 microstructure were seen. It was observed that grain growth has occurred, but relatively low at lower content of zirconia (10 wt.%). However, with the increase of the additive

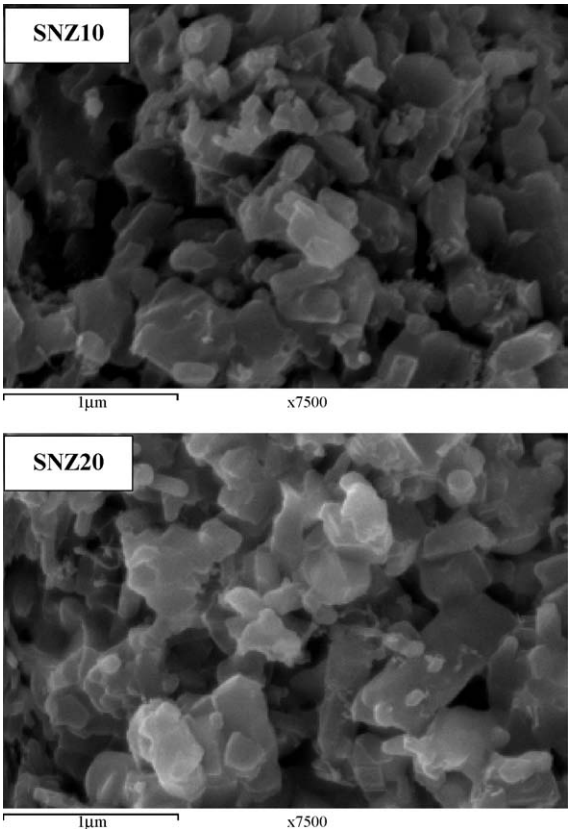

Fig. 4. SEM micrographs of group I (fracture surface). With the increase of ZrO_2 addition, aspect ratio and grain growth of the silicon nitride increases. This is a good evidence on the transformation of α-Si_3N_4 to β-Si_3N_4.

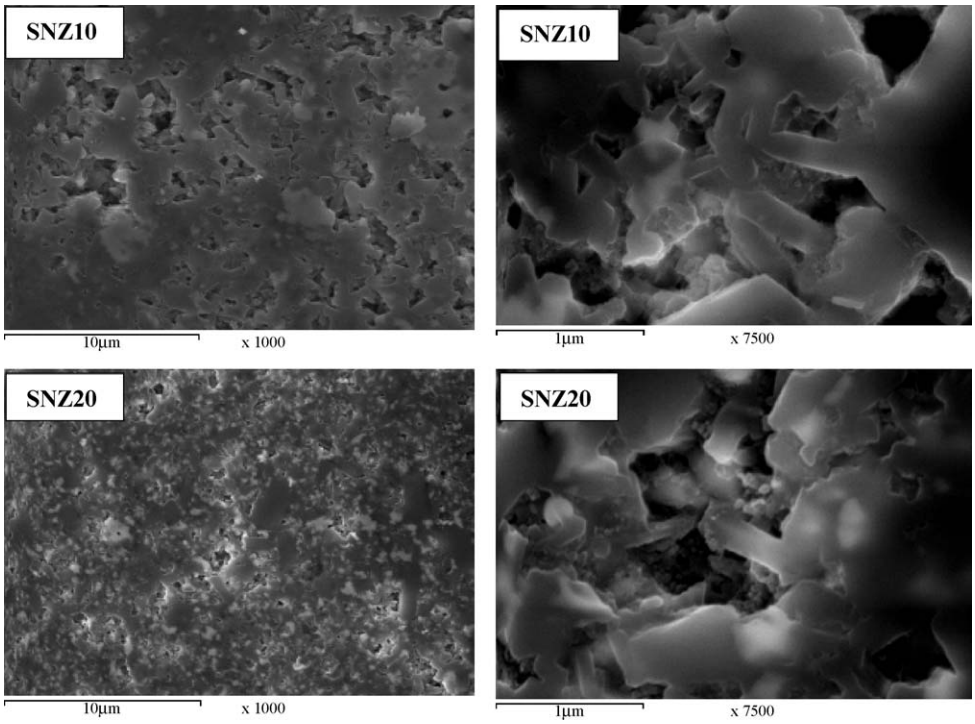

Fig. 5. SEM micrographs of HP-samples of group I (polished surface with different magnification). It can be seen that (a) ZrO_2 (light grains) is well-distributed in Si_3N_4 matrix, (b) irregular pores are very clear and there content and its sizes decrease with increase of ZrO_2 content, and (c) no complete densification at low content of ZrO_2 (SNZ10) and there is enhancement with increasing the content of ZrO_2 (SNZ20).

amount up to 20 wt.% zirconia, the grains were significantly larger. In addition, the volume fraction of elongated grains increased. These observations affirm that the aspect ratio of the grains in the hot-pressed samples increased with the increase of the amount of zirconia. This in turns indicates the formation of β-silicon nitride and matches with the X-ray results. However, the formation of β-silicon nitride is not evidence for the complete densification. Fig. 5 shows the effect of the amount of sintering additives on the densification and microstructure of group (I) samples (only ZrO_2 additives). At low content of ZrO_2 (SNZ10), a large volume of irregular pores are evident. With the increase of ZrO_2 addition (SNZ20), the porosity decreases. This indicates that densification of Si_3N_4 improves with increasing zirconia content but even with 20 wt.% zirconia full density is not achieved. Incomplete densification is most likely due to either low volume fraction of the liquid phase or due to high viscosity of the liquid phase.

Addition of mixtures of zirconia and alumina to equimolecular mixtures from α- and β-Si_3N_4 represented in group (II) had significant changes on the microstructure of the hot-pressed samples as shown in Fig. 6 (low and high magnification). SEM of the hot-pressed samples of this group shows an improvement in the densification. However, it appears that the amount of liquid phase formed with addition of 10 wt.% zirconia and alumina with ratio 1:1 (SNZA1) seems to be insufficient to form a high density composite. By increasing the amount of zirconia and alumina mixture to 20 wt.% content with same ratio (SNZA2), the crystalline phases are uniform and well-distributed in the matrix. From the microstructure feature, the liquid phase formed seems to be enough and leads to a dense composite. SEM of hot-pressed silicon nitride samples (SNZA3 and SNZA4) containing zirconia/alumina ratio of 0.5 (Z/A = 0.5) for both 10 or 20 wt.% exhibited uniform and well-distributed microcrystalline phases embedded in the amorphous matrix. This microstructure indicates near full density materials. The important conclusion from these results is that both the amount of liquid phase and its state or chemistry is important in controlling the hot-pressing process. When Z/A ratio was increased to 2 (i.e. Z/A = 2) as in samples SNZA5, uniform crystalline and microcrystalline phases embedded in the matrix were observed at low content of the additives (10 wt.%). In addition, pores were observed indicating incomplete densification. With the increase of the content to 20 wt.% at the same ratio (Z/A = 2) as in samples SNZA6, a uniform and well-distributed microcrystalline phase embedded in liquid phase was observed without residual porosity. An eutectic liquid of low viscosity at the processing temperature is formed in the ZrO_2–Al_2O_3 system at $Z/A < 1$. Increasing of the Z/A ratio to 2 means increasing the amount of ZrO_2 which in turn increases the viscosity. Incompleted densification results for this case. These results affirm that such effective densification mainly depend on the amount of liquid formed and its state.

3.2. Densification

Silicon nitride samples without addition of sintering additives have been called ‘‘unsinterable’’ due to the difficulties

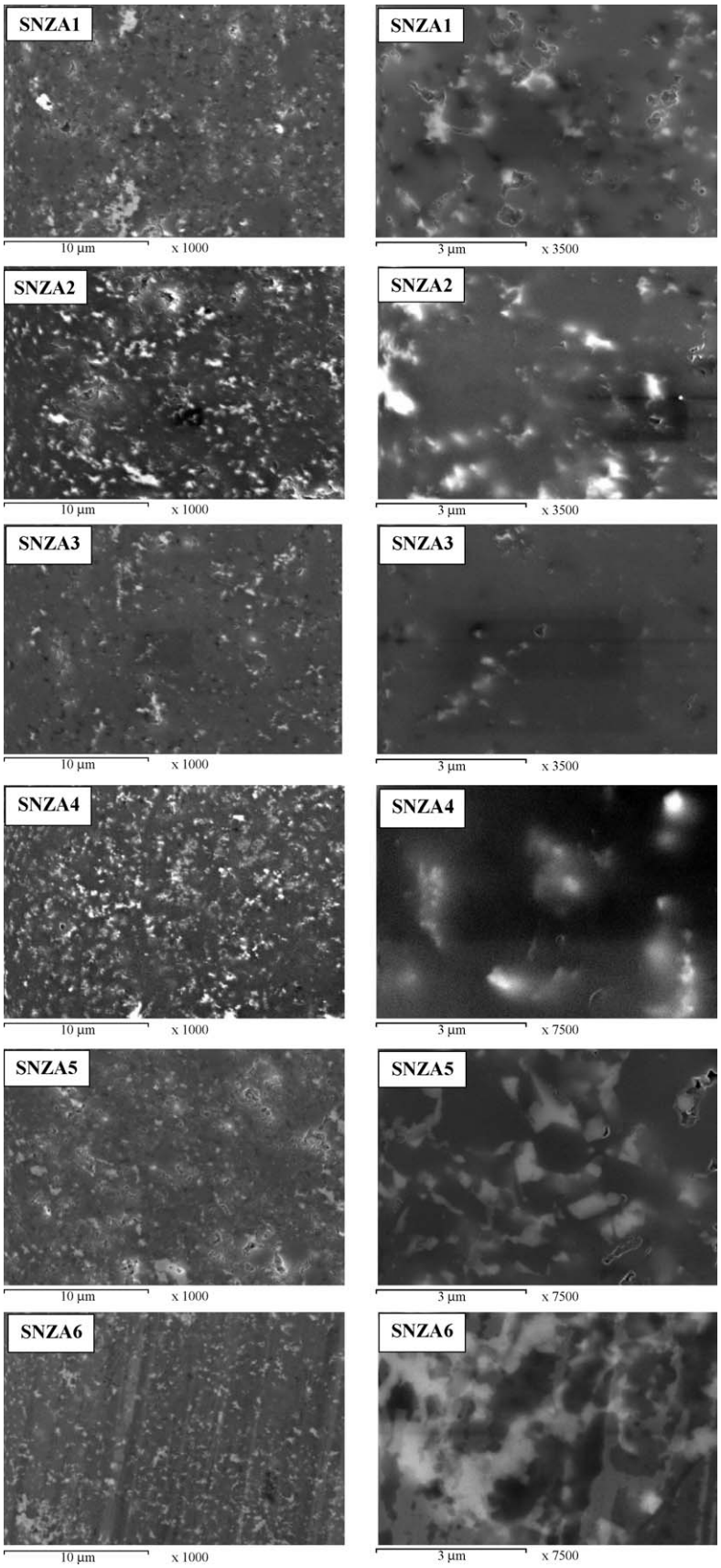

Fig. 6. SEM micrographs of group II (polished surface with low and high magnification). It can be seen that (1) light area corresponds to ZrO_2, (2) two features are clears in the figures and proved by EDS; (a) *main part of ZrO_2 is separated in the form of damaged grains and well-distributed in the matrix*, *and* (b) *the other part ZrO_2 (minor) forms eutectic mixtures with Al_2O_3 and well-distributed in the grey area*, (3) Black area or spots have been confirmed to be referred to glassy phase

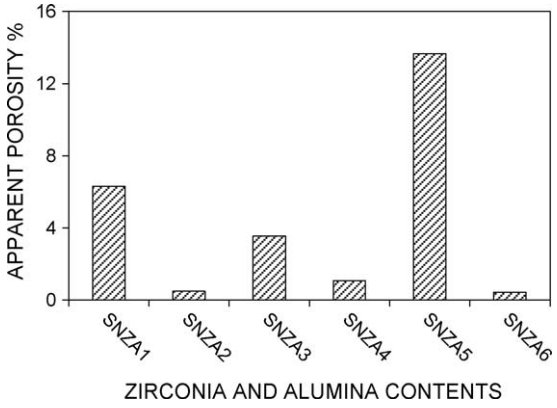

Fig. 7. Bulk density of hot-pressed Si_3N_4 as a function of ZrO_2 content.

Fig. 8. Apparent porosity of hot-pressed Si_3N_4 as a function of ZrO_2 content.

associated with sintering ''pure'' Si_3N_4 [9,23,28]. However, the addition of zirconia and zirconia/alumina to equimolecular mixtures of α- and β-Si_3N_4 resulted in improved densification for the composites. The final densities depend on the amount and type of the additives.

In case of the hot-pressed silicon nitride mixtures of group (I) which contains 5–20 wt.% zirconia, the densification parameters in terms of bulk density and apparent porosity of the sintered samples are presented in Figs. 7 and 8. These figures displayed that the average bulk density of the hot-pressed samples increased with increasing amount of zirconia. Despite the increase of the density of the hot-pressed samples, it is still low compared to the expected density of the hot-pressed Si_3N_4. These low densities may be due to insufficient amount of liquid phase formed during hot-pressing process [14–16,24,28,33,36,42,63–65,74–76]. In addition, the formations of Si_2N_2O phase in these mixtures during the sintering process as seen in the XRD (Fig. 1) led to poor sinterability. Since the addition of zirconia to silicon nitride produced high apparent porosity and low bulk density, therefore, the manufacturing of fully dense-pore free silicon nitride composites from this mixture cannot be obtained under the hot-pressing conditions used.

The bulk density and apparent porosity of the hot-pressed silicon nitride mixtures of group (II) which contains 10 and 20 wt.% zirconia(Z)/alumina(A) of different ratios (1, 0.5 and 2) is shown in Figs. 9 and 10. Generally, the apparent porosity of the hot-pressed silicon nitride mixtures of the group (II) was lower for all cases (whatever the content or ratios of zirconia and alumina) compared to group (I). Key factor in the decrease of the apparent porosity of this group can be understood from the Al_2O_3–ZrO_2 phase diagram [50]. In this diagram, the composition of Z/A = 0.5 forms a eutectic at 1710 ± 10 °C. With increasing Z/A ratio, the liquidus temperature increases leading to an increase in the viscosity of the liquid at the processing temperature. It has also been shown that the surface

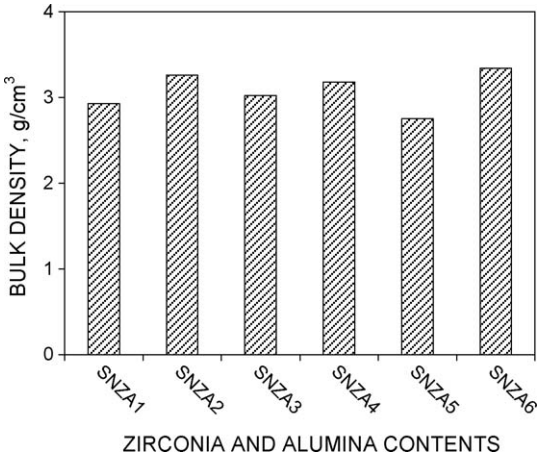

Fig. 9. Bulk density of hot-pressed Si_3N_4 as a function of ZrO_2 and Al_2O_3 mixtures cat different contents and ratios.

tension of the liquid that forms at Z/A = 0.5 is a minimum [77,78]. With the increase of the ratios of Z/A, the surface tension of the liquid increases up to ratio of 4 then decreases again. Thus the liquid that forms at Z/A = 0.5, has lower surface tension and consequently easily wets the grains. It also has the low viscosity at the processing temperature. This in turn assists the packing of the grains by rearrangement and decreases the porosity. In addition to the low surface tension of the liquid, the quantity of the liquid is also important. For that reasons, 20 wt.% from Z/A = 0.5 gave pore free structure. At higher content and Z/A ratio of 0.5 and 1, the liquid formed has low enough surface tension and viscosity and this leads to dense samples. When the Z/A ratio is 2, the surface tension increases and also the liquidus temperature increases leading to samples that are no longer fully dense. Thus in addition to the amount of liquid, the liquidus temperature and the surface tension are

composed mainly of aluminum silicate. Other part of alumina has been found in the grey areas and the ratio of Z/A is less than 1, (4) Si_3N_4 is cemented by two kind of liquid phase [amorphous mullite and amorphous liquid of ZrO_2–Al_2O_3 composite with Z/A < 1], and (5) most of samples show compacting with high content of Z/A irrespective to the ratio, however, glassy-like feature was seen with samples of Z/A = 0.5 (SNZA3and SNZA4) indicating complete densification and the role of liquids feature.

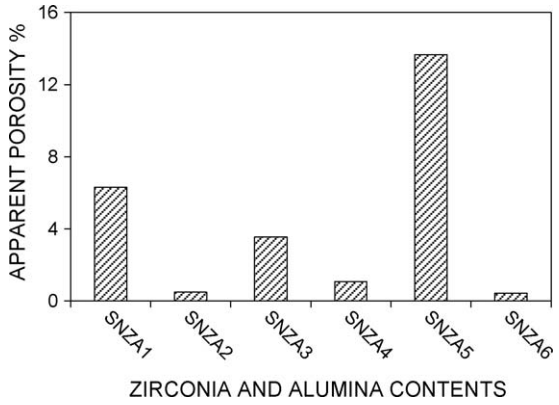

Fig. 10. Apparent porosity of hot-pressed silicon nitride as a function of ZrO_2 and Al_2O_3 mixtures at different contents and ratios.

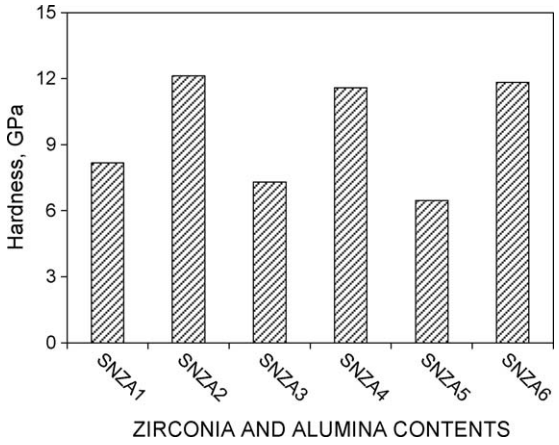

Fig. 12. Vickers hardness of hot-pressed Si_3N_4 as a function of ZrO_2 and Al_2O_3 mixtures at different contents and ratios.

important factors in controlling densification of liquid phase sintered materials.

3.3. Mechanical properties

3.3.1. Hardness

Hardness of the hot-pressed Si_3N_4 samples containing zirconia additives ''group (I)'' determined by Vickers indentation didn't show any change up to 15 wt.% zirconia additions as shown in Fig. 11. These hardness values are quite low compared to the hardness of silicon nitride found in literature. The low hardness is due to relatively low density and the high content of β-Si_3N_4 [17,24,60,74,79]. With the increase of the content of zirconia to 20 wt.%, the hardness value increased significantly. This can be explained by the decrease in porosity and increasing of density. However, this value is still low compared to the results reported for silicon nitride.

For the hot-pressed Si_3N_4 mixtures of group (II), the hardness values, displayed in Fig. 12, show remarkable improvement. In spite of the difference in the hardness among the mixtures, the results are in good agreement with results found in the literature. Significant increase in the hardness of the samples (SNZA2, SNZA4 and SNZA6) of high zirconia and alumina content (20 wt.%) was observed compared to the samples (SNZA1, SNZA3 and SNZA5) containing low content of additives (10 wt.%). This was true irrespective to the ratio of Z/A. This most likely is due to the low porosity of the material as discussed above. This observation is in agreement with reported literature [17,24,60,65,73,79–81].

3.3.2. Fracture toughness

Hot-pressed silicon nitride samples of group (I) which contains zirconia only gave palmqvist crack according to (*C*/*a*) ratio results. By applying the indentation fracture equation of palmqvist crack [52,55,61], it was found that the fracture toughness (K_{IC}) of the hot-pressed samples of this group increased with increasing amount of zirconia as shown in Fig. 13. The increase of K_{IC} might be due to the transformation of zirconia from tetragonal to monoclinic under cooling from sintering temperature to room temperature [3,10,11,38,82–85]. The starting zirconia powder was tetragonal and the zirconia obtained in the sintered samples is monoclinic as seen by XRD. The increase of β-Si_3N_4 formed with high aspect ratio generated from the conversion of α-Si_3N_4 to β-Si_3N_4 as seen by SEM could be another reason contributing to the improvement of K_{IC}, where, the presence of such kind of

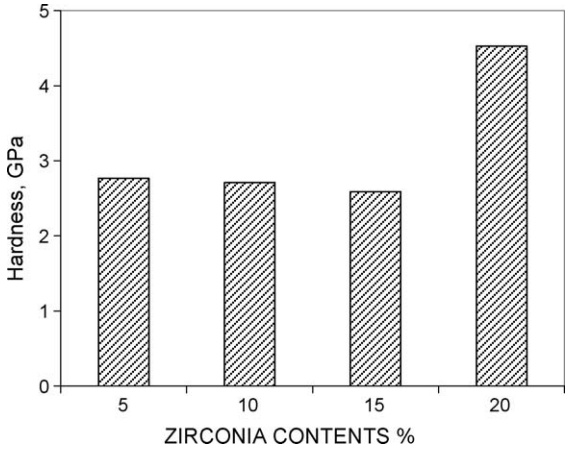

Fig. 11. Vickers hardness of hot-pressed Si_3N_4 as a function of ZrO_2 content.

Fig. 13. Fracture toughness of hot-pressed Si_3N_4 as a function of ZrO_2 content.

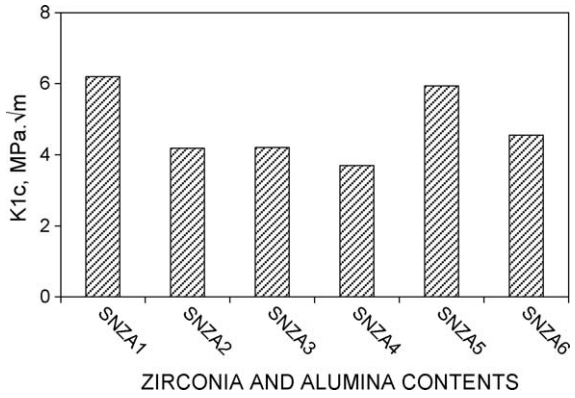

Fig. 14. Fracture toughness of hot-pressed Si_3N_4 as a function of ZrO_2 and Al_2O_3 mixtures at different contents and ratios.

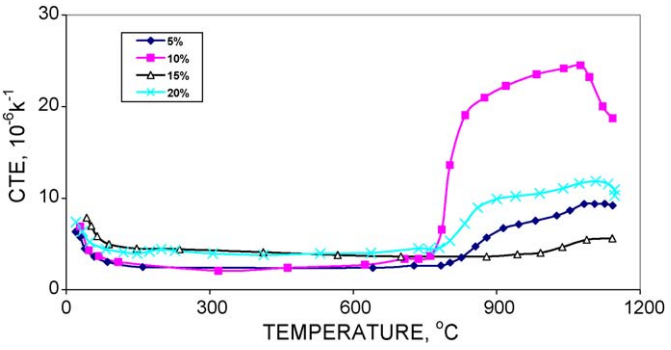

Fig. 16. Coefficient of thermal expansion of hot-pressed Si_3N_4 as a function of ZrO_2 content.

elongated texture deflects the propagation of cracks. In addition, thermal expansion mismatch between silicon nitride and zirconia could be contributing in the increase of the fracture toughness of the hot-pressed samples [4,74,86]. Despite the significant improvement in the fracture toughness (K_{IC}) of the hot-pressed samples of this group, the values are quite low compared to K_{IC} of silicon nitride found in literature. This difference could be understood in term of the large amount of porosity that is present in these samples.

According to (*C*/*a*) ratios results, hot-pressed silicon nitride samples of group (II) gave two patterns of cracks. The samples containing 10 wt.% of zirconia and alumina mixtures, for all Z/A ratios (SNZA1, SNZA3 and SNZA5) gave palmqvist crack, while the samples containing 20 wt.% (SNZA2, SNZA4 and SNZA6) gave half penny crack. By applying the indentation fracture equation for the appropriate crack type, K_{IC} of the hot-pressed samples were obtained and are shown in Fig. 14. These results are in good agreement with those reported in literature [87–89]. Also, the presence of higher content of β-Si_3N_4 with elongated grains enhances the fracture toughness due to the mechanism of crack bridging of the elongated grains [15,16,17,24,38,42,58,73–75,78–80,90–92]. An additional factor that contributed to the improvement of the fracture toughness is thermal expansion mismatch between the matrix and reinforcing the particle. This mismatch leads to residual stresses which promote crack deflection and the formation of crack bridging [4,74,86].

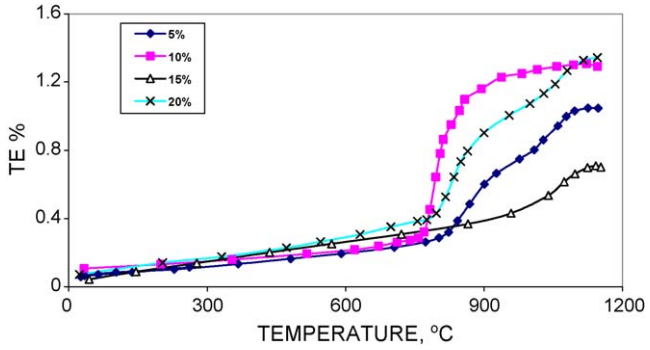

Fig. 15. Thermal expansion of hot-pressed Si_3N_4 as a function of ZrO_2 content.

3.4. Thermal properties

Figs. 15 and 16 show the linear thermal expansion (TE) and its coefficient (CTE) of the hot-pressed samples "group (I)" material (containing only ZrO_2 additives) as a function of temperature. The TE increases linearly with temperature (constant CTE) of this group up to 800 °C. With the increase of ZrO_2 content, TE and CTE increased because ZrO_2 has high TE and CTE when compared to Si_3N_4 [3,93]. However, with increasing the temperature above 800 °C, a deviation from the linear trend of TE is observed. This may be due to the softening of the glassy grain boundary phases [73]. In addition, zirconia phase changes from monoclinic to tetragonal during heating [9,10,38,81–84]. This transformation is martensitic in nature [9,10,94,95] and involves a finite volume change (4–5%).

Figs. 17 and 18 show TE and CTE of hot-pressed Si_3N_4 mixtures of group (II) as a function of temperature. Generally, TE and CTE of the hot-pressed samples containing ZrO_2 and Al_2O_3 mixture of this group gave a lower thermal expansion than the samples containing only ZrO_2. Hot-pressed samples containing 10 and 20 wt.% of Z/A = 0.5 (SNZA3 and SNZA4) gave negative thermal expansion (NTE) over temperature range starting from room temperature up to 1100 °C and these values are considered the lowest values obtained. The characteristics

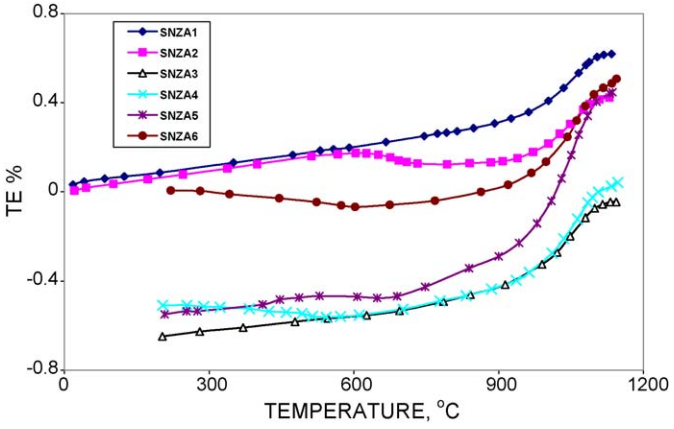

Fig. 17. Thermal expansion of hot-pressed Si_3N_4 as a function of ZrO_2 and Al_2O_3 mixtures at different contents and ratios.

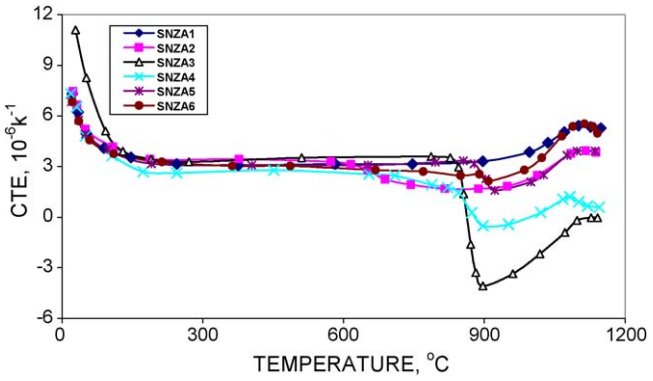

Fig. 18. Coefficient of thermal expansion of hot-pressed Si_3N_4 as a function of ZrO_2 and Al_2O_3 mixtures at different contents and ratios.

of the formed liquid composition could explain the observed NTE. Low or negative thermal expansion coefficient is attractive for a number of interesting applications. At Z/A = 2, the hot-pressed samples (SNZA5) containing 10 wt.% showed negative TE and CTE up to 1000 °C. However, with addition 20 wt.% (SNZA6), NTE was obtained in temperature of range starting from room temperature up to 850 °C. Appearance of some crystalline phases in this composition as discussed in microstructure section and decreasing of the content of liquids was considered as a reason. Comparing these results with the results of the hot-pressed samples containing zirconia alumina mixtures of Z/A = 0.5 (SNZA3 and SNZA4), NTE is considered low. The reason maybe the appearance of some crystalline phases in this composition as discussed in the microstructure section and the decrease in the content of the liquid phase. Finally, for equal amounts of zirconia and alumina (SNZA1 and SNZA2), i.e. Z/A = 1 whatever the amount added in the frame of this study, NTE was not observed. This can be explained in terms of the nature of the liquid phase formed and the crystalline microstructure observed.

4. Conclusions

The study of the effect of the additions of ZrO_2 and ZrO_2/Al_2O_3 on the hot-pressing of the equimolecular mixture from α- and β-Si_3N_4 revealed that it is difficult to manufacture dense or near fully dense silicon nitride object with addition of zirconia only. However, near-full density samples were obtained by the addition of ZrO_2 and Al_2O_3. The amount of and the type of liquid phase, in addition to its quantity are proposed as important parameter in controlling the densification during the hot-pressing of silicon nitride. A significant observation is the importance of using eutectics in the phase diagram as effective ways for achieving high density.

Addition of zirconia only did not show significant improvement in the mechanical properties in terms of both hardness and fracture toughness (K_{IC}) and these properties were considered quite low compared to those reported in the literature. However, addition of 20 wt.% zirconia and alumina mixtures, for all Z/A ratio, investigated gave good mechanical properties in term of hardness but the specimen containing 10 wt.% zirconia and alumina mixtures, for all Z/A ratios investigated gave high K_{IC}.

Samples containing Z/A ratios 0.5 and 2 exhibited negative thermal expansion (NTE) for both 10 and 20 wt.% additives. However, the specimen containing Z/A of 1 showed positive thermal expansion. NTE is very useful for a range of applications and further research should be conducted to understand and optimize this behavior.

Acknowledgements

The authors would like to thank Prof. Oleg N. Grigoriev and Prof. George V. Lashkarev at the Institute for Problems of Materials Science, NAS of Ukraine, for helping in hot-pressing of the samples.

References

[1] S.M. Sapuan, M.S.D. Jacob, F. Mustapha, N. Ismail, A prototype knowledge-based system for material selection of ceramic matrix composites of automotive engine components, Mater. Des. 23 (2002) 701–708.
[2] M. Bengisu, Engineering Ceramics, Springer Verlag, Berlin, Heidelberg, Germany, 2001, pp. 28–30, 358, 407–444.
[3] H. Schilp, Fabrication of turbine-compressor-shaft assembly for micro gas turbine engine, M.Sc. Thesis, Rapid Prototyping Laboratory Stanford University and Institute for Metal Forming and Casting Technische Universität München, December 2000.
[4] R.E. Smallman, R.J. Bishop, Modern Physical Metallurgy and Materials Engineering, 6 ed., Butterworth-Heinemann, London, England, 1999, pp. 320–334.
[5] M.N. Rahaman, Ceramic Processing and Sintering, Marcel Dekker Inc, MO, USA, 1995, pp. 1–5 and 331–371.
[6] C.A. Harper, Handbook of Materials for Product Design, 3 ed., McGraw-Hill Professional, USA, 2001.
[7] R.W. Cahn, Encyclopedia of Materials Science and Technology, Elsevier Science, UK, 2001.
[8] H.O. Pierson, Handbook of Refractory Carbides and Nitrides Properties, Characteristics, Processing and Applications, Noyes Publications, Westwood, New Jersey, 1996, pp. 2 and 209–326.
[9] B. Basu, Toughening of yttria-stabilised tetragonal zirconia ceramics, Int. Mater. Rev. 50 (2005) 239–256.
[10] B. Basu, J. Vleugels, O. Van Der Biest, Transformation behavior of yttria stabilized tetragonal zirconia polycrystal–TiB_2 composites, J. Mater. Res. 16 (2001) 2158–2169.
[11] W.H. Tuan, T.C. Chen, C.H. Wang, Mechanical properties of Al_2O_3/ZrO_2 composites, J. Eur. Ceram. Soc. 22 (2002) 2827–2833.
[12] R. Koc, S. Kaza, Synthesis of α-Si_3N_4 from carbon coated silica by carbothermal reaction and nitridation, J. Eur. Ceram. Soc. 18 (10) (1998) 1471–1477.
[13] W.T. Lo, J.L. Huang, Z.H. Shih, The effects of ytterbium oxide on the microstructure and R-curve behaviors of silicon nitride, Mater. Chem. Phys. 73 (2002) 123–128.
[14] J.G. Fisher, S.K. Woo, K. Bai, Microwave reaction bonding of silicon nitride using an inverse temperature gradient and ZrO_2 and Al_2O_3 sintering additives, J. Eur. Ceram. Soc. 23 (2003) 791–799.
[15] G. Ling, H. Yang, Pressureless sintering of silicon nitride with magnesia and yttria, Mater. Chem. Phys. 90 (1) (2005) 31–34.
[16] Y. Sun, Q. Menga, D. Jia, Effect of hexagonal BN on the microstructure and mechanical properties of Si_3N_4 ceramics, Mater. Proc. Technol. 182 (1–3) (2007) 134–138.
[17] V. Biasini, S. Guicciardi, A. Bellosi, Silicon nitride–silicon carbide composite materials, Refract. Met. Hard Mater. 11 (1992) 213–221.

[18] J. Dai, J. Li, Y. Chen, Effect of the residual phases in β-Si_3N_4 seed on the mechanical properties of self-reinforced Si_3N_4 ceramics, J. Eur. Ceram. Soc. 23 (2003) 1543–1547.
[19] X. Xu, L. Huang, X. Liu, Effects of α/β ratio in starting powder on microstructure and mechanical properties of silicon nitride ceramics, Ceram. Int. 28 (2002) 279–281.
[20] S. Ogata, N. Hirosaki, C. Kocer, A comparative study of the ideal strength of single crystal α- and β-Si_3N_4, Acta Mater. 52 (2004) 233–238.
[21] C.J. Lee, J.I. Chae, D.J. Kim, Effect of β-Si_3N_4 starting powder size on elongated grain growth in β-Si_3N_4 ceramics, J. Eur. Ceram. Soc. 20 (14–15) (2000) 2667–2671.
[22] Y.C. Kim, C.H. Kim, D.K. Kim, Effect of microwave heating on densification and α → β phase transformation of silicon nitride, J. Eur. Ceram. Soc. 17 (13) (1997) 1625–1630.
[23] A. Vuckovic, S. Boskovic, B. Matovic, Effect of β-Si_3N_4 seeds on densification and fracture toughness of silicon nitride, Ceram. Int. 32 (2006) 303–307.
[24] A.D. Pablos, M.I. Osendi, P. Miranzo, Correlation between microstructure and toughness of hot pressed Si_3N_4 ceramics seeded with β-Si_3N_4 particles, Ceram. Int. 29 (2003) 757–764.
[25] M. Kitayama, K. Hirao, M. Toriyama, Modeling and simulation of grain growth in Si_3N_4-II. The α-β transformation, Acta Mater. 46 (1998) 6551–6557.
[26] L. Bonnie, A. Turner, N. Naresh, Shock-enhanced alpha to beta phase transformation in Si_3N_4 powders, Mater. Sci. Eng. A256 (1998) 289–300.
[27] D.J. Baxter, T. Graziani, H.M. Wang, Corrosion of a dense, low-additive Si_3N_4 in high temperature combustion gases, J. Eur. Ceram. Soc. 18 (16) (1998) 2323–2330.
[28] X.J. Liu, Z.Y. Huang, Q.M. Ge, Microstructure and mechanical properties of silicon nitride ceramics prepared by pressureless sintering with MgO–Al_2O_3–SiO_2 as sintering additive, J. Eur. Ceram. Soc. 25 (14) (2005) 3353–3359.
[29] G.A. Swift, Neutron diffraction study of in situ-reinforced silicon nitride during creep, Ph.D., California Institute of Technology Pasadena, California, March 2004.
[30] S. Guo, N. Hirosaki, Y. Yamamoto, Hot-pressed silicon nitride ceramics with Lu_2O_3 additives: elastic moduli and fracture toughness, J. Eur. Ceram. Soc. 23 (3) (2003) 537–545.
[31] V. Demir, D.P. Thompson, Vacuum heat treatment of $LiAlO_2$ densified silicon nitride ceramics, Mater. Des. 27 (2006) 1102–1107.
[32] R. Kleina, V. Medrib, M.D. Bruta, Influence of additives content on the high temperature oxidation of silicon nitride based composites, J. Eur. Ceram. Soc. 23 (4) (2003) 603–611.
[33] E.D. Whitney, Ceramic Cutting Tools Material Development, and Performance, Noyes Publications, Florida, USA, 1994, pp. 191–220.
[34] A.G. King, Ceramic Technology and Processing, Noyes publication, William Andrew Publishing: Norwich, New York, 2002, pp. 134–175, 231–290 and 336.
[35] H.J. Choi, J.G. Lee, High temperature strength and oxidation behaviour of hot-pressed silicon nitride-disilicate ceramics, Mater. Sci. 32 (1997) 1937–1942.
[36] J.G.P. Binner, Advanced Ceramic Processing and Technology, Noyes Publications, New Jersey, USA, 1990, pp. 39–71.
[37] Z. Tatli, D.P. Thompson, Low temperature densification of silicon nitride materials, J. Eur. Ceram. Soc. 27 (2007) 791–795.
[38] B.T. Lee, H.D. Kim, Effect of sintering additives on the nitridation behavior of reaction-bonded silicon nitride, Mater. Sci. Eng. A364 (2004) 126–131.
[39] H. Kaya, The application of ceramic-matrix composites to the automotive ceramic gas turbine, Compos. Sci. Technol. 59 (1999) 861–872.
[40] H.T. Lin, M.K. Ferber, Mechanical reliability evaluation of silicon nitride ceramic components after exposure in industrial gas turbines, J. Eur. Ceram. Soc. 22 (14–15) (2002) 2789–2797.
[41] M.P. Albano, L.B. Garrido, A.B. Garcia, Dispersion of aluminum hydroxide coated Si_3N_4 powders with ammonium polyacrylate dispersant, Colloids Surf. A: Physicochem. Eng. Aspects 181 (2001) 69–78.
[42] Y.I. Lee, Y.W. Kim, Effects of additive amount on microstructure and mechanical properties of silicon carbide–silicon nitride composites, Mater. Sci. 36 (2001) 699–702.
[43] J. Weiss, L.J. Gauckler, T.Y. Tien, The system Si_3N_4–SiO_2–ZrN–ZrO_2, J. Am. Ceram. Soc. 62 (11–12) (1979) 632–634.
[44] C.S. Lee, K.S. Lee, S. Lee, D.K. Kim, Effect of grain boundary phase on contact damage resistance of silicon nitride ceramics, Key Eng. Mater. 287 (2005) 421–426.
[45] L.K.L. Falk, Microstructure and short-term oxidation of hot-pressed $Si_3N_4/ZrO_2(+Y_2O_3)$ ceramics, J. Am. Ceram. Soc. 75 (1) (1992) 28–35.
[46] B. Lee, T. Koyama, A. Nishiyama, K. Hiraga, Microstructure and fracture characteristic of Si_3N_4–ZrO_2 (MgO) ceramic composite studied by transmission electron microscopy, Scripta Metall. Mater. 32 (7) (1995) 1037–1077.
[47] F. Sigulinski, B. Boskovic, Phase composition and fracture toughness of Si_3N_4–ZrO_2 with CeO_2 additions, Ceram. Int. 25 (1999) 41–47.
[48] T. Ekstroem, L.K.L. Falk, E.M. Knutson-Wedel, Pressureless-sintered Si_3N_4–ZrO_2 composites with Al_2O_3 and Y_2O_3 additions, J. Mater. Sci. Lett. 9 (7) (1990) 823–826.
[49] T. Ekstroem, L.K.L. Falk, E.M. Knutson-Wedel, Si_3N_4–ZrO_2 composites with small Al_2O_3 and Y_2O_3 additions prepared by HIP, J. Mater. Sci. Lett. 26 (1991) 4331–4340.
[50] G. Cevales, System ZrO_2–Al_2O_3, Ber. Dtsch. Keram. Ge. 45 (5) (1968) 216–219.
[51] ASTM C1327-03: Test method for vickers indentation hardness of advanced ceramics, Annual book of ASTM standards, Section 15, vol. 15.01, ASTM, West Conshohocken, PA, 2006.
[52] F. Sergejev, M. Antonov, Comparative study on indentation fracture toughness measurements of cemented carbides, Proc. Estonian Acad. Sci. Eng. 12 (2006) 388–398.
[53] K.K. Bamzai, P.N. Kotru, B.M. Wanklyn, Investigations on indentation induced hardness and fracture mechanism in flux grown DyAlO crystals, Appl. Surf. Sci. (133) (1998) 195–204.
[54] H.J. Yount, Hardness and fracture toughness of heat treated advanced ceramic materials for use as fuel coating and inert matrix materials in advanced reactors, M.Sc., University of Wisconsin Madison, 2006.
[55] H.R. Lawn, E.R. Fuller, Equilibrium penny-like cracks in indentation fracture, J. Mater. Sci. 10 (1975) 2016–2024.
[56] I. Sevim, M.K. Kulekci, Abrasive wear behaviour of bio-active glass ceramics containing apatite, Bull. Mater. Sci. 29 (2006) 243–249.
[57] J. Wang, J. Gong, Z. Guan, Variation in the indentation toughness of silicon nitride, Mater. Lett. (57) (2002) 643–646.
[58] H. Miyazaki, H. Hyuga, K. Hirao, T. Ohji, Comparison of fracture resistance as measured by the indentation fracture method and fracture toughness determined by the single-edge-precracked beam technique using silicon nitrides with different microstructures, J. Eur. Ceram. Soc. 27 (6) (2007) 2347–2354.
[59] S. Guo, Hot pressed silicon nitride ceramics with Lu_2O_3 additives: elastic moduli and fracture toughness, J. Eur. Ceram. Soc. 23 (3) (2003) 537–545.
[60] A. Mukhopadhyay, B.S. Basu, Das Bakshi, S.K. Mishra, Pressureless sintering of ZrO_2–ZrB_2 composites: microstructure and properties, Int. J. Refract. Met. Hard Mater. 25 (2007) 179–188.
[61] M. Albakry, M. Guazzato, M.V. Swain, Fracture toughness and hardness evaluation of three pressable all-ceramic dental materials, J. Dent. 31 (2003) 181–188.
[62] S. Ordonez, The influence of amount and type of additives on β → β Si_3N_4 transformation, Mater. Sci. 34 (1999) 147–153.
[63] S. Wada, P. Chaiypak, S. Jinawath, Sintering of Si_3N_4 ceramics in air atmosphere furnace (part 2)—agglomeration of packing powder and deterioration of Al_2O_3 crucible, J. Ceram. Soc. Jpn. 112 (2004) 234–237.
[64] M.J. Hoffmann, A. Geyer, R. Oberacker, Potential of the sinter-HIP-technique for the development of high-temperature resistant Si_3N_4 ceramics, J. Eur. Ceram. Soc. 19 (13–14) (1999) 2359–2366.
[65] H. Hyuga, M.I. Jones, K. Hirao, Microstructural characteristics in silicon nitride/tungsten composites by different in situ processing, Mater. Lett. 58 (2003) 21–24.
[66] E. Narimatsu, Y. Shinoda, T. Akatsu, F. Wakai, Effect of chemical composition of intergranular glass on superplastic compressive deformation of β-silicon nitride, J. Eur. Ceram. Soc. 26 (6) (2006) 1069–1074.
[67] M. Ohashi, K. Nakamura, K. Hirao, Factors affecting mechanical properties of silicon oxynitride ceramics, Ceram. Int. (23) (1997) 27–37.

[68] R.G. Duan, G. Roebben, J. Vleugels, In situ formation of Si_2N_2O and TiN in Si_3N_4-based ceramic composites, Acta Mater. (53) (2005) 2547–2554.
[69] M. Radwan, T. Kashiwagi, Y. Miyamoto, New synthesis route for Si_2N_2O ceramics based on desert sand, J. Eur. Ceram. Soc. 23 (2003) 2337–2341.
[70] N. Pradeilles, M.C. Record, R.M. Marin, A modified SHS method for Si_2N_2O elaboration, J. Eur. Ceram. Soc. 26 (2006) 2489–2495.
[71] Q. Tong, J. Wang, Z. Li, Low-temperature synthesis/densification and properties of Si_2N_2O prepared with Li_2O additive, J. Eur. Ceram. Soc. 27 (2007) 4767–4772.
[72] S.P. Taguchi, S. Ribeiro, Silicon nitride oxidation behaviour at 1000 and 1200 °C, Mater. Proc. Technol. 147 (2004) 336–342.
[73] F. Monteverde, S. Guicciardi, A. Bellosi, Advances in microstructure and mechanical properties of zirconium diboride based ceramics, Mater. Sci. Eng. A346 (2003) 310–319.
[74] S.A. Baldacim, C. Santos, O.M.M. Silva, Mechanical properties evaluation of hot-pressed Si_3N_4–$SiC_{(w)}$composites, Int. J. Refract. Met. Hard Mater. 21 (2003) 233–239.
[75] C.C. Liu, Microstructural characterization of gas-pressure-sintered α silicon nitride containing β-phase seeds, Ceram. Int. 29 (2003) 841–846.
[76] J.P. Sancho, J.A. Pero-Sanz, L.F. Verdeja, Toughness of Si_3N_4 ceramics obtained by precipitating sintering aids as hydroxides, Mater. Charact. 50 (2003) 11–22.
[77] V.E. Deutscher, Slag Atlas, 2 ed., Verlag Stahleisen GmbH, Germany, September 1995, pp. 49 and 417.
[78] Z. Zhao, L. Zhang, Y. Song, W. Wang, J. Wu, Microstructures and properties of rapidly solidified Y_2O_3 doped Al_2O_3/ZrO_2 composites prepared by combustion synthesis, Scripta Mater. 55 (9) (2006) 819–822.
[79] C. Santos, K. Strecker, S.A. Baldacim, Mechanical properties improvement related to the isothermal holding time in Si_3N_4 ceramics sintered with an alternative additive, Int. J. Refract. Met. Hard Mater. 21 (2003) 245–250.
[80] M. Nakamura, K. Hirao, Y. Yamauchi, Wear behaviour of α-Si_3N_4 ceramics reinforced by rod-like β-Si_3N_4 grains, Wear 254 (2003) 94–102.
[81] S.A. Baldacim, C.A.A. Cairo, C.R.M. Silva, Mechanical properties of ceramic composite, Mater. Proc. Technol. 119 (2001) 273–276.
[82] C. Tian, N. Liu, M. Lu, Thermal shock and thermal fatigue behavior of Si_3N_4–TiC nano-composites, Int. J. Refract. Met. Hard Mater. 26 (5) (2008) 478–484.
[83] N.C. Biswas, S.P. Chaudhuri, Effect of thermal-shock and autoclave treatment on the microstructure of $A1_20_3$–ZrO_2 composite, Ceram. Int. 23 (1997) 69–72.
[84] G.Y. Lin, T.C. Lie, Microstructure, mechanical properties and thermal shock behaviour of $A1_2O_3 + ZrO_2 + SiC_w$ composites, Ceram. Int. 24 (1998) 313–326.
[85] N.M. Rendtorff, L.B. Garrido, E.F. Aglietti, Thermal shock behavior of dense mullite–zirconia composites obtained by two processing routes, Ceram. Int. 34 (2008) 2017–2024.
[86] F. Ye, L. Liu, J. Zhang, Synthesis of silicon nitride-barium aluminosilicate self-reinforced ceramic composite by a two-step pressureless sintering, Compos. Sci. Technol. 65 (2005) 2233–2239.
[87] S. Guo, N. Hirosaki, Y. Yamamoto, T. Nishimura, M. Mitomo, Hot-pressed silicon nitride ceramics with Lu_2O_3 additives: elastic moduli and fracture toughness, J. Eur. Ceram. Soc. 23 (3) (2003) 537–545.
[88] B. Mikijelj, J. Mangels, E. Belfield, A. MacQueen, Silicon Nitride Applications in Modern Diesel Engines, SAE International, http://www.sae.or/technical/papers/2004-01-1448.
[89] D. Stienstra, Introduction to design of structural cearmics, Ph.D., Mechanical Engineering, Rose-Hulman Institute of Technology, terre Haute, Indiana, Copyright 1992 revised 2003.
[90] O. Penas, R. Zenati, J. Dubois, Processing, microstructure, mechanical properties of Si_3N_4 obtained by slip casting and pressureless sintering, Ceram. Int. 27 (5) (2001) 591–596.
[91] Y. Chiang, D.P. Birnie, W.D. Kingery, Physical Ceramics (Principles for Ceramic Science and Engineering), New York, Wiley, 1997.
[92] C.P. Dogan, J.A. Hawk, Microstructure and abrasive wear in silicon nitride ceramics, Wear 250 (2001) 256–263.
[93] M. Kalantar, C. Fantozzi, Thermo-mechanical properties of ceramics: resistance to initiation and propagation of crack in high temperature, Mater. Sci. Eng. 472 (2008) 273–280.
[94] M. Yoshimura, Phase stability of zirconia, Am. Ceram. Soc. Bull. 67 (1988) 1950–1955.
[95] A.M. Alper, High-Temperature Oxides, Part II, Academic Press, New York, 1970, 126 pp.